World Applied Sciences Journal 13 (7): 1748-1756, 2011
ISSN 1818-4952

Radiation Effects on MHD Boundary Layer Stagnation Point Flow Towards a Heated Shrinking Sheet

Muhammad Ashraf and Shahzad Ahmad

Centre for Advanced Studies in Pure and Applied Mathematics,
Bahauddin Zakariya University, Multan, Pakistan

Abstract: A comprehensive study of MHD two dimensional boundary layer stagnation point flow with radiation effects towards a heated shrinking sheet immersed in an electrically conducting viscous incompressible fluid in the presence of a transverse magnetic field is analyzed numerically. The governing continuity, momentum and heat equations together with the associated boundary conditions are first reduced to a set of self similar non linear ordinary differential equations and are then solved by a method based on finite difference discretization. Some important features of the flow and heat transfer in terms of normal and horizontal velocities and temperature distributions for different values of the governing parameters are analyzed, discussed and presented through tables and graphs. The present investigations predict that the reverse flow caused due to shrinking of the sheet can be stopped by applying a strong magnetic field. The magnetic field enhances the shear stresses and decreases the thermal boundary layer thickness. The heat loss per unit area from the sheet decreases with an increase in the shrinking parameter. The thermal boundary layer becomes thinner with increasing values of the radiation parameter. The present results may be beneficial in flow and thermal control of polymeric processing.

Key words: MHD stagnation flow · Heat transfer · Shrinking sheet · Radiation · Finite differences

INTRODUCTION

MHD stagnation point flows with heat transfer effects have applications in many manufacturing processes in industry. These applications include boundary layer along material handling conveyers, the aerodynamics extrusion of plastic sheets, blood flow problems, the cooling of an infinite metallic plate in a cooling bath and textile and paper industries.

The classical two dimensional stagnation point flow on a flat plate was first studied by Hiemenz [1]. The numerical study of laminar steady two dimensional flow over a semi infinite permeable flat surface with mass and heat transfer at the wall was considered by Chamkha and Issa [2]. The governing equations of motion were reduced into ordinary ones using a similarity transformation. An implicit tridiagonal finite difference scheme was used to solve the reduced self similar equations. Mahapatra and Gupta [3] investigated numerically the steady two dimensional stagnation point flow of an electrically conducting power law fluid over a stretched surface. Roslinda *et al.* [4] presented the numerical study of unsteady boundary layer flow of an incompressible viscous fluid in the stagnation point region over a stretching sheet. Keller box method was used to solve the boundary layer equations. The problem of steady two dimensional laminar MHD mixed convection stagnation point flow with mass transfer over a heated permeable surface was examined by Abdelkhalek [5]. Coupled non linear partial differential equations were solved by using perturbation technique. A numerical study of two dimensional boundary layer stagnation point flow over a stretching sheet in case of injection/ suction through porous medium with heat transfer was considered by Layek *et al.* [6]. Anuar *et al.* [7] considered the numerical study of steady stagnation point flow on a vertical surface through a porous medium. The governing partial differential equations were first reduced to ordinary differential equations using similarity transformation and the resulting equations were then solved using Keller box method. The numerical solution of MHD steady laminar two dimensional stagnation flow of a viscous

Corresponding Author: Muhammad Ashraf, Centre for Advanced Studies in Pure and Applied Mathematics, Bahauddin Zakariya University, Multan, Pakistan. E-mail: mashraf_mul@yahoo.com.

incompressible electrically conducting fluid of variable thermal conductivity over a stretching sheet was obtained by Sharma and Singh [8]. The governing equations of motion were reduced into ordinary differential equations using similarity transformation. The reduced ordinary differential equations were then solved using shooting method. Stagnation point flow with convective heat transfer towards a shrinking sheet was investigated by Wang [9]. Mahapatra *et al*. [10] investigated numerically the steady two dimensional stagnation point flow of an electrically conducting power law fluid over a stretched surface in the presence of a magnetic field. Two dimensional stagnation point flow in a porous medium was studied by Kumaran *et al*. [11]. Perturbation technique was used to obtain series solution of governing equations. Kumaran *et al*. [12] studied the problem of MHD boundary layer flow of an electrically conducting fluid over a stretching and permeable sheet with injection/ suction through the sheet. The problem of similarity solutions of the effect of variable viscosity on unsteady mixed convection boundary layer flow over a vertical surface embedded in a porous medium was discussed by Hamad and Muatazz [13] by using HAMAD formulations. Hayat *et al*. [14] considered the MHD stagnation point flow and heat transfer through a porous space bounded by a permeable surface. The governing partial differential equations were first reduced to ordinary differential equations using similarity transformation and the resulting equations were then solved using HAM. The numerical study of steady two dimensional laminar forced MHD Hiemenz flow over a flat plate in a porous medium was solved by Kechil and Hashim [15] using implicit scheme method. Two dimensional magnetohydrodynamic oscillatory flow along a uniformly moving infinite vertical porous plate bounded by porous medium was studied by Ahmad and Ahmad [16]. Kuo [17] investigated the problem of thermal boundary layer in a semi-infinite flat plate using differential transformation method. The effect of radiation on the flow and heat transfer over a wedge with variable viscosity was presented numerically by Elbashbeshy *et al*. [18]. The effect of thermal radiation on the natural convection flow along a uniformly heated vertical porous plate with variable viscosity and uniform suction velocity was studied numerically by Hossain *et al*. [19]. The effects of thermal radiation on the laminar boundary layer about a flat-plate were discussed by Bataller [20] and presented the effects of Prandtl number and radiation parameter. Bhuvaneswari *et al*. [21] studied the problem of convection and mass transfer of a viscous electrically conducting incompressible fluid over a semi infinite inclined plane in a porous medium with radiations and heat generation.

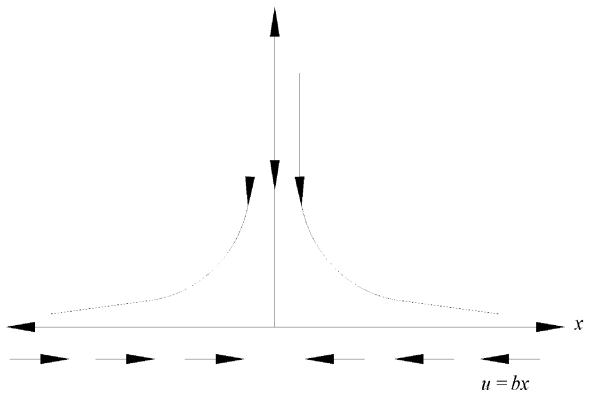

Fig. 1: A sketch of the physical problem

The aim of the present study is to investigate radiation effects on MHD two dimensional stagnation point flow of a steady viscous incompressible electrically conducting fluid towards a shrinking sheet in the presence of a transverse magnetic field.

Problem Formulation: Consider two dimensional MHD stagnation point flow of an electrically conducting fluid impinging normally on a heated shrinking sheet as shown in Figure (1). The flow is assumed to be laminar, steady, viscous and incompressible. We assume that the uniform stationary magnetic field of strength B_0 is perpendicular to the velocity field V. The magnetic Reynolds number is assumed to be small Shercliff [22] so that the induced magnetic field can be neglected as compared to the imposed field. We assume that there is no applied polarization voltage, so the electric field is zero. Further we assume that the Boussinesq and boundary layer approximations are valid. The equations of motion for two dimensional steady viscous incompressible boundary layer flow of an electrically conducting fluid, can be written as

$$\frac{\partial u}{\partial x}+\frac{\partial v}{\partial y}=0 \tag{1}$$

$$u\frac{\partial u}{\partial x}+v\frac{\partial u}{\partial y}=-\frac{1}{\rho}\frac{\partial p}{\partial x}+\frac{\mu}{\rho}\frac{\partial^2 u}{\partial y^2}+\frac{\sigma_e B_0{}^2}{\rho}(U-u), \tag{2}$$

Here ρ is the density of the fluid, p is the pressure, σ_e is the electric conductivity of the fluid and U is the free stream velocity of the fluid.

The equation for temperature distribution for the present boundary value problem, neglecting the viscous dissipation, can be written as

$$\rho\, c_p\left(u\frac{\partial T}{\partial x}+v\frac{\partial T}{\partial y}\right)=\kappa_0\frac{\partial^2 T}{\partial y^2}-\frac{\partial q_r}{\partial y} \tag{3}$$

Where T is the temperature, κ_0 is the constant thermal conductivity, c_p is the specific heat capacity at constant pressure of the fluid and q_r is the radiative heat flux.

Using the Rosseland approximation for radiation Raptis *et al.* [23], the radiative heat flux is simplified as

$$q_r=-\frac{4\sigma}{3k}\frac{\partial T^4}{\partial y}, \tag{4}$$

Where k and σ are the Stefan–Boltzmann constant and the mean absorption coefficient, respectively. We assume that the temperature differences within the flow such as that the term T^4 may be expressed as a linear function of temperature. Hence, expanding T^4 in a Taylor series about T^∞ and neglecting higher-order terms we get

$$T^4\cong 4T^3{}_\infty\, T-3T^4{}_\infty \tag{5}$$

In view of Equations (4) and (5), Equation (3) reduces to

$$u\frac{\partial T}{\partial x}+v\frac{\partial T}{\partial y}=\left(\frac{k_0}{\rho c_p}+\frac{16\sigma T^3{}_\infty}{3\rho c_p k}\right)\frac{\partial^2 T}{\partial y^2} \tag{6}$$

From the above equation it is seen that the effect of radiation is to enhance the thermal conductivity. If we take $Nr=\frac{kk_0}{4\sigma T^3{}_\infty}$ as the radiation parameter, Equation (6) becomes.

$$u\frac{\partial T}{\partial x}+v\frac{\partial T}{\partial y}=\frac{\alpha_0}{k}\frac{\partial^2 T}{\partial y^2} \tag{7}$$

Where $k=\frac{3Nr}{3Nr+4}$.

The boundary conditions for the velocity and temperature fields for the problem under consideration can be written as.

$$\left.\begin{aligned}&u(x,0)=bx, v(x,0)=0, u(x,\infty)=U=ax,\\&T(x,0)=T_0, T(x,\infty)=T_\infty.\end{aligned}\right] \tag{8}$$

Here $b > 0$ is the shrinking rate, T_0 is the heated surface temperature and T_∞ is the temperature of the fluid outside the boundary layer ($T_0 > T_\infty$). In order to obtain the velocity and temperature fields for our problem, we have to solve Equations (1) and (2) and Equation (7) subject to the appropriate boundary conditions given in Equation (8). For this we use following similarity transformations.

$$\left.\begin{aligned}&\eta=\sqrt{\frac{a}{\upsilon}}y,\ p(x,\infty)=p_0-\frac{\rho a^2}{2}(x^2+y^2),\\&u(x,y)=axf'(\eta),\ v(x,y)=-\sqrt{a\upsilon}f(\eta),\\&\theta(\eta)=\frac{T-T_\infty}{T_0-T_\infty}.\end{aligned}\right] \tag{9}$$

Where η is similarity parameter, P_0 is the stagnation pressure, a is the strength of stagnation point having dimension of $\frac{1}{t}$.

Using Equation (9) in Equation (1), we note that equation of continuity (1) is identically satisfied and therefore the velocity field represents the possible fluid motion. Using Equation (9) in Equation (2) and after a little simplification, we get.

$$f'''+M^2(1-f')+1=f'^2-ff'' \tag{10}$$

Again using Equation (9) in Equation (7) we get,

$$\theta''+Prkf\theta'=0. \tag{11}$$

Here $M=\sqrt{\frac{\sigma_e B_0{}^2}{\rho a}}$ and $Pr=\frac{\mu c_p}{\kappa_0}$ are Hartmann number (or magnetic parameter) and Prandtl number respectively. Where $k=\frac{3Nr}{3Nr+4}$ and Nr is radiation parameter.

Boundary conditions given in Equation (8) in view of Equation (9) can be written as.

$$\left.\begin{aligned}&f(0)=0, f'(0)=b/a=B, f'(\infty)=1,\\&\theta(0)=1, \theta(\infty)=0.\end{aligned}\right] \tag{12}$$

NUMERICAL SOLUTION

The governing equations (10) and (11) are highly non linear. Most of the physical systems are inherently non linear in nature and are of great interest to physicists, engineers and mathematicians. Problems involving non linear ordinary differential equations are difficult to solve and give rise to interesting phenomina such as chaos. We use a finite difference based numerical algorithm to solve present boundary value problem comprising the coupled non linear differential Equations (10) and (11) and boundary conditions (12). Following Chamkha and Issa [2] and Ashraf *et al.* [24-26], we reduce the order of the Equation (10) by one with the help of substitution $q = f'$ such that Equation (10) and the boundary conditions given in Equation (12) becomes as follows.

$$q = f' = \frac{df}{d\eta} \tag{13}$$

$$q'' + M^2(1-q) + 1 = q^2 - fq' \tag{14}$$

$$\left.\begin{aligned} &f(0) = 0, q(0) = B, q(\infty) = 1, \theta(0) = 1, \\ &\theta(\infty) = 0. \end{aligned}\right] \tag{15}$$

We have to solve the Equations (11), (13) and (14) subject to the boundary conditions (15). For numerical solution of the present problem we first discretize the domain (0, ∞) uniformly with step h. Equation (13) is integrated using Simpson's rule Gerald [27] with the formula given in Milne [28]. Equations (11) and (14) are discretized at a typical grid point $\eta = \eta_n$ of the interval (0, ∞) by employing central difference approximations for the derivatives and then are solved iteratively by Successive over relaxation (SOR) method Hildebrand [29], subject to the appropriate boundary conditions given in Equation (15). In order to accelerate the iterative procedure, to improve the accuracy of the solution and to have an estimate of local as well as global discretization errors, we use the solution procedure which is mainly based on algorithm described by Syed *et al.* [30]. The iterative process is stopped if the following criterion is satisfied for the three consecutive iterations.

$$\text{Max}\,(\|q^{(k+1)} - q^{(k)}\|_2, \|f^{(k+1)} - f^{(k)}\|_2,$$

$$\|\theta^{(k+1)} - \theta^{(k)}\|_2,) < TOL_{iter} \tag{16}$$

Here TOL_{iter} is the prescribed error tolerance and we have taken at least 10^{-12} for our calculations during the execution of a computer program.

The higher order accuracy of the approximations to the exact solutions can be obtained by the use of Richardson's extrapolation. This process can be carried out using any extrapolation scheme Deuflhaard [31].

RESULTS AND DISCUSSION

This section is devoted for the presentation of our findings in tabular and graphical form. In order to develop a better understanding of the physics of the problem, we choose to present the effects of shear stresses, the shrinking parameter, the magnetic parameter, the radiation parameter and the Prandtl number on the flow and heat transfer characteristics. For the stability of our numerical scheme and to improve the order of accuracy of the solutions, numerical results are computed for three grid sizes and then are extrapolated using Richardson's extrapolation. It is important to note that the for numerical solutions, the value of η_∞ depends on the non dimensional parameters which govern the problem. We have adjusted η_∞ in order to have asymptotic behavior of velocity and temperature profiles. A comparison of numerical values of temperature velocity $\theta(\eta)$ for the three grid sizes $h, \frac{h}{2} \& \frac{h}{4}$ and their extrapolated values is shown in Table (1). Excellent comparisons validate our numerical computations. Table (2) is another source of validity of the present results in which our results compare well with the literature results of Lok [32] and Wang [9]. Table (3) gives values of shear stress $f''(0)$ and heat transfer

Table 1: Dimensionless temperature profiles $\theta(\eta)$ on the three grid levels and extrapolated values for B=–0.5,M = 1.0, Nr = 3.0, Pr = 0.7 and $\eta_\infty = 6$.

	$\theta(\eta)$			
η	h	$\frac{h}{2}$	$\frac{h}{4}$	Extrapolated values
0	1	1	1	1
0.6	0.772112	0.771656	0.771313	0.771177
1.2	0.546686	0.545984	0.545386	0.54515
1.8	0.346008	0.345302	0.344627	0.344359
2.4	0.192431	0.191896	0.191319	0.191087
3	0.092947	0.092629	0.092239	0.092081
3.6	0.038632	0.038483	0.038272	0.038186
4.2	0.013665	0.013612	0.013519	0.013481
4.8	0.004006	0.003992	0.00396	0.003947
5.4	0.000861	0.000859	0.000852	0.000849
6	0	0	0	0

Table 2: Comparison of the present results with the literature results given by Lok [32] and Wang [9] with M = 0, Nr = 0, Pr = 0.7 & η_∞ = 5

	$f''(0)$		
B	Present	Wang [9]	Lok [32]
0.20	1.05112	1.05113	1.05129
0.50	0.71328	0.71330	0.71334

Table 3: Shear stresses and heat transfer rate for M = 1, Nr = 3.0, Pr = 0.7 and η_∞ = 6 with various values of B.

–B	$f''(0)$	$-\theta'(0)$
0.25	1.877455	0.412803
0.50	2.120114	0.378822
0.75	2.307090	0.342202
1.0	2.429972	0.302334
1.25	2.476343	0.258227
1.50	2.425917	0.208447
1.75	2.239347	0.149512
2.0	1.805761	0.076282

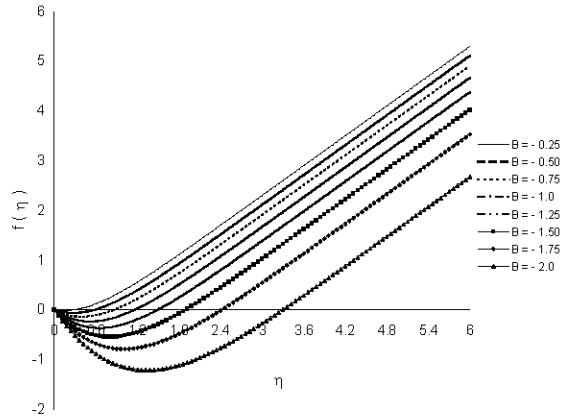

Fig. 2: Normal velocity profiles for M = 1, Nr = 3.0, Pr = 0.7 and η_∞ with various values of B.

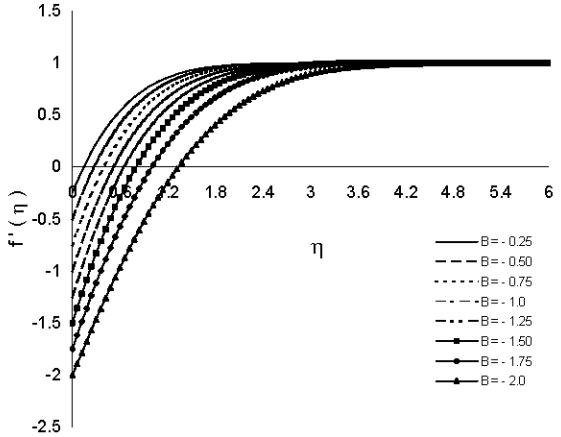

Fig. 3: Horizontal velocity profiles for M = 1, Nr = 3.0, Pr = 0.7 and Pr = 0.7 and η_∞ with various values of B.

rate $-\theta'(0)$ at the sheet for various values of shrinking parameter B in the presence of weak transverse magnetic field (M = 1), the shear stress increases for $0.25 \le -B \le 1.25$. However, a reverse trend can be seen for $1.25 < -B \le 2.0$. This non monotonic behavior of shear stress against the shrinking parameter has also been reported by Wang [9] in the absence of magnetic filed. Physically this behaviour may be attributed to the fact that vertical growth rate of horizontal flow reversal region and hence of boundary layer thickness is not uniform with increase in B as may be seen in the horizontal velocity profiles sketched in Figure (3). As the horizontal flow reversal causes vertical flow reversal in the vicinity of the stagnation point, for larger values of B extents of vertical flow regime increase as shown in Figure (2) and complex interaction of vertical flow reversal and impinging flow causes the boundary layer thickness grow rapidly, thus reducing the shear

Table 4: Shear stresses and heat transfer rate for B =–0.5, Nr = 3.0, Pr = 0.7 and η_∞ = 5 with various values of M.

M	$f''(0)$	$-\theta'(0)$
0.0	1.495722	0.346172
0.5	1.674222	0.356736
1.0	2.120137	0.379832
1.5	2.703497	0.405899
2.0	3.353283	0.432773
2.5	4.037486	0.460611
3.0	4.741092	0.489584

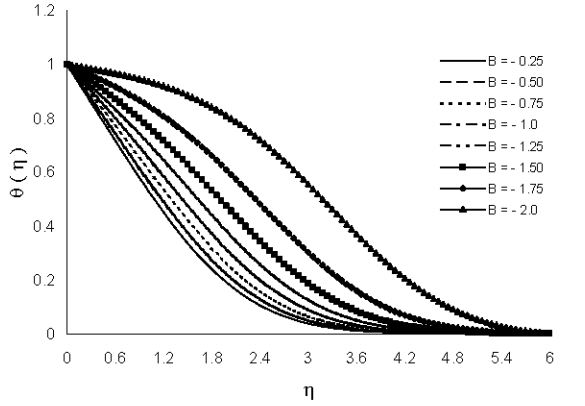

Fig. 4: Temperature profiles for M = 1, Nr = 3.0, Pr = 0.7 and η_∞ with various values of B.

stress at the shrinking surface. The heat loss per unit area from the sheet decreases by increasing the magnitude of shrinking parameter B which is the consequence of horizontal flow reversal resulting into reduced convection rate.

Table (4) predicts the influence of applied magnetic field on the shear stress and heat transfer rate. The shear stress and heat transfer rate from the surface increase with an increase in the magnetic parameter M. This is because the transverse magnetic field assists the impinging flow and reduces horizontal and vertical flow reversal as may be seen in the normal and horizontal velocity profiles shown in Figures (5) and (6).

The effect of the radiation parameter Nr on heat transfer $-\theta'(0)$ is given in Table (5). The heat transfer from the heated sheet to the fluid increases as Nr is increased. However, the effect of Nr is less significant for its larger values. This is natural as the heat loss at the heated surface is now determined by two modes of heat transfer the conduction and the radiation. Increasing the values of radiation parameter thus enhances the heat transfer rate. From Table (6) it is noted that the loss of heat transfer increases for all values of the Prandtl number Pr in the given range. Figures (2), (3) and (4) illustrate the effect of the shrinking parameter B on the velocity and

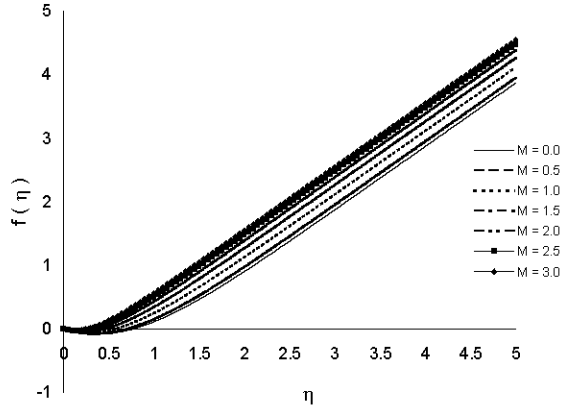

Fig. 5: Normal velocity profiles for $B = 0.5$, $Nr = 3.0$, $Pr = 0.7$ and $\eta_\infty = 5$ with various values of M.

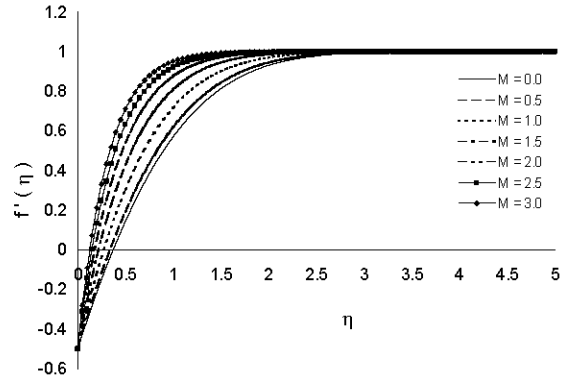

Fig. 6: Horizontal velocity profiles for $B = 0.5$, $Nr = 3.0$, $Pr = 0.7$ and $\eta_\infty = 5$ with various values of M.

Table 5: Heat transfer rate for $B = -0.5$, $M = 1.0$, $Pr = 0.7$ and $\eta_\infty = 6$ with various values of Nr

Nr	$-\theta'(0)$
0.7	0.305083
2.0	0.361612
4.0	0.388843
6.0	0.400024
8.0	0.406115
10.0	0.409946
100.0	0.424983
200.0	0.425881
300.0	0.426182
400.0	0.426333
500.0	0.426423
600.0	0.426484
700.0	0.426527
800.0	0.426559
900.0	0.426584
1000.0	0.426605

Table 6: Heat transfer rate for $B = -0.5$, $M = 1.0$, $Nr = 3.0$ and $\eta_\infty = 6$ with various values of Pr

Pr	$-\theta'(0)$
0.1	0.236814
0.2	0.266021
0.3	0.292959
0.4	0.317579
0.5	0.339977
0.6	0.360324
0.7	0.378822
0.8	0.395683
0.9	0.411109
1.0	0.425282

temperature fields. It can be noted from Figure (2) that normal velocity profiles $f(\eta)$ decrease with the increase in magnitude of B. Figure (3) plots the horizontal velocity $f'(\eta)$ for different values of B. The horizontal velocity profiles decrease as the magnitude of shrinking rate increases. The temperature at a point rises with an increase in the shrinking rate as shown in Figure (4). The velocity and thermal boundary layers become thicker by increasing the magnitude of the shrinking parameter as shown in Figures (3) and (4). This trend of velocity and temperature profiles is obviously due to the horizontal and vertical flow reversal caused by the shrinking of the sheet which increase with increasing the shrinking rate. This flow reversal hinders heat, mass and momentum transfer from sheet to fluid as also reported by Wang [9].

The influence of imposition of the magnetic field on the velocity and temperature fields is predicted in Figures (5), (6) and (7). The normal and horizontal velocity profiles rise as the magnetic parameter M increases. As noted earlier, the magnetic field assists the impinging flow and, therefore, reduces the extents of horizontal and vertical flow reversal regimes and causes the hydrodynamic and thermal boundary layers thickness to decrease and become thinner. In this way transverse magnetic field can effectively be used to counteract the effects of shrinking with its strength adjusted according to the rate at which the sheet shrinks.

Figure (8) predicts the influence of the radiation parameter Nr on the temperature field. The temperature profiles fall as Nr is increased. Further the thinning of the thermal boundary layer occurs by increasing the values of Nr as shown in Figure (8). This is due to the high convection rate enriched by taking into account the radiative heat flux. These results dictate that radiative mode of heat transfer can be employed to enhance the surface heat loss.

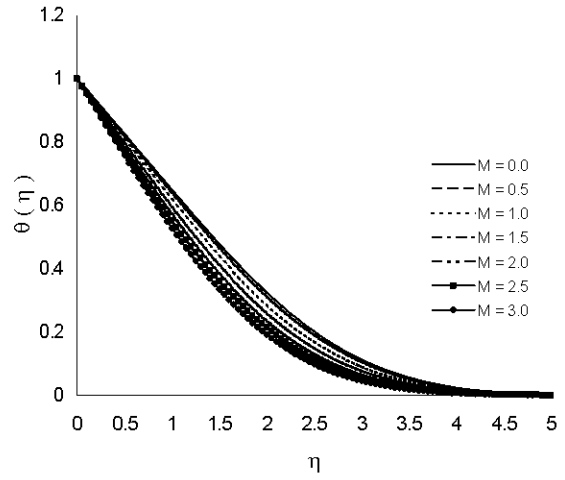

Fig. 7: Temperature profiles for $B = 0.5$, $Nr = 3.0$, $Pr = 0.7$ and $\eta_\infty = 5$ with various values of M.

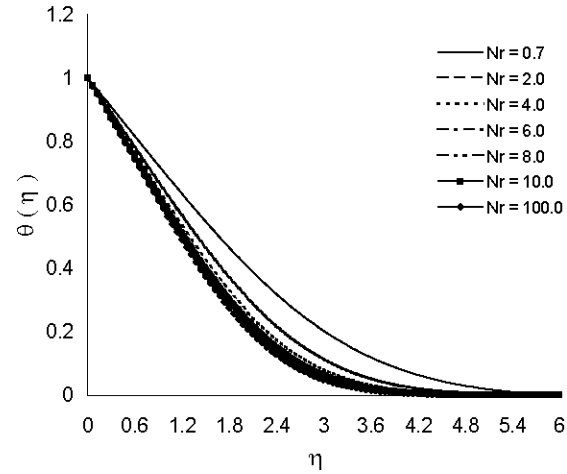

Fig. 8: Temperature profiles for $B = 0.5$, $Nr = 3.0$, $Pr = 0.7$ and $\eta_\infty = 5$ with various values of Nr.

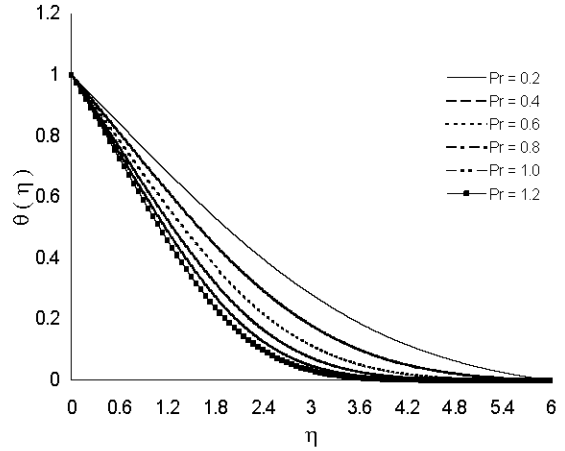

Fig. 9: Temperature profiles for $B = 0.5$, $Nr = 3.0$, $Pr = 0.7$ and $\eta_\infty = 5$ with various values of Pr.

Finally, Figure (9) displays the influence of the Prandtl number Pr on the fluid temperature. It can be concluded that the temperature at a point decreases with an increase in Pr. The thermal boundary layer thickness decreases by increasing values of Pr.

CONCLUSIONS

This study considered the effects of shrinking parameter, magnetic parameter, radiation parameter and Prandtl number on two dimensional laminar steady viscous incompressible stagnation point flow and heat transfer of an electrically conducting fluid towards a heated shrinking sheet. The transformed self similar equations with associated boundary conditions were solved numerically by an algorithm based on finite differences. The following conclusions can be made.

- A region of reverse flow occurs near the surface of the sheet due to the shrinking rate and can be stopped by applying a strong magnetic field.
- The velocity and thermal boundary layers become thicker with an increase in the values of shrinking parameter and become thinner by increasing the magnetic field.
- The heat loss per unit area from the sheet decreases with an increase in the magnitude of shrinking parameter.
- The presence of the thermal radiation term in the energy equation reduces the temperature distribution.
- The thermal boundary layer decreases by increasing the value of radiation parameter.

ACKNOWLEDGEMENT

The authors wish to express their very sincere thanks to the reviewers for their valuable suggestions to improve the quality of the paper.

REFERENCES

1. Hiemenz, K., 1911. Die Grenzschicht an einem in den gleichformingen Flussigkeitsstrom eingetauchten graden Kreiszylinder. Dinglers Polytechnic J., 326: 321-324.
2. Chamkha, A.J. and C. Issa, 2000. Effects of heat generation/ absorption and thermophoresis on hydromagnetic flow with heat and mass transfer over a flat surface. Int. J. Numer. Methods Heat Fluid Flow, 10: 432-49.

3. Mahapatra, T.R. and A.S. Gupta, 2001. MHD stagnation point flow towards a stretching sheet. Acta Mechanica, 152: 191-196.
4. Roslinda, N., N. Amin, D. Filip and I. Pop, 2004. Unsteady boundary layer flow in the region of the stagnation point on a stretching sheet. Int. J. Eng. Sci., 42: 1241-1253.
5. Abdelkhalek, M.M., 2006. The skin friction in the MHD mixed convection stagnation point with mass transfer. International Communications in Heat and Mass Transfer, 33: 249-258.
6. Layek, G.C., S. Mukhopadhyay and S.A. Samad, 2007. Heat and mass transfer analysis for boundary layer stagnation point flow towards a heated porous stretching sheet with heat absorption/ generation and suction / blowing. International Communications in Heat and Mass Transfer, 34: 347-356.
7. Anuar, I., N. Roslinda and I. Pop, 2008. Dual solutions in mixed convection flow near a stagnation point on a vertical surface in a porous medium. International J. Heat and Mass Transfer, 51: 1150-1155.
8. Sharma, P.R. and G. Singh, 2008. Effects of variable thermal conductivity and heat source/ sink on MHD flow near a stagnation point on a linearly stretching sheet. J. Appl. Fluid Mechanics, 2: 13-21.
9. Wang, C.Y., 2008. Stagnation flow towards a shrinking sheet. International J. Non Linear Mechanics, 43: 377-382.
10. Mahapatra, T.R., S.K. Nandy and A.S. Gupta, 2009. MHD stagnation point flow of a power law fluid towards a stretching surface. International J. Non Linear Mechanics, 44: 124-129.
11. Kumaran, V., R. Tamizharasi and K. Vajravelu, 2009. Approximate analytic solutions of stagnation point flow in a porous medium. Communications in Non Linear Science and Numerical Simulation, 14: 2677- 2688.
12. Kumaran, V., A.K. Banerjee, A. Vanav Kumar and K. Vajravelu, 2009. MHD flow past a stretching permeable sheet. Applied Mathematics and Computation, 210: 26-32.
13. Hamad, M.A.A. and M.A. Bashir, 2011. Similarity Solutions of the Effect of Variable Viscosity on Unsteady Mixed Convection Boundary Layer Flow over a Vertical Surface Embedded in a Porous Medium via HAMAD Formulations. World Appl. Sci. J., 12(4): 519-530.
14. Hayat, T., T. Javed and Z. Abbas, 2009. MHD flow of a micropolar fluid near a stagnation point towards a non linear stretching surface. J. Porous Media, 12: 183-195.
15. Kechil, S. and I. Hashim, 2009. Approximate analytical solution for MHD stagnation point flow in porous media. Communications in Non Linear Science and Numerical Simulation, 14: 1346-1354.
16. Ahmad, S. and N. Ahmad, 2004. Two dimensional magnetohydrodynamic oscillatory flow along a uniformly moving infinite vertical porous plate bounded by porous medium. Indian J. Pure and Appl. Math., 35(12): 1309-1319.
17. Kuo, B.L., 2004. Thermal boundary-layer problems in a semi-infinite flat plate by the differential transformation method. Appl. Mathematics and Computation, 150: 303-320.
18. Elbashbeshy, E.M.A. and M.F. Dimian, 2002. Effect of radiation on the flow and heat transfer over a wedge with variable viscosity. Appl. Mathematics and Computation, 132: 445-454.
19. Hossain, T.M.A., K. Khanafer and K. Vafai, 2001. The effect of radiation on free convection flow of fluid with variable viscosity from a porous vertical plate. Int. J. Therm. Sci., 40: 115-124.
20. Bataller, R.C., 2008. Radiation effects in the Blasius flow. Applied Mathematics and Computation, 198: 333-338.
21. Bhuvaneswari, M., S. Sivasankaran and Y.J. Kim, 2010. Exact analysis of radiation convective flow heat and mass transfer over an inclined plate in a porous medium. World Appl. Sci. J., 10(7): 774-778.
22. Shercliff, J.A., 1965. A text book of magnetohydrodynamics, *Pergamon Press*, Oxford.
23. Raptis, A., C. Perdikis and H.S. Takhar, 2004. Effect of thermal radiation on MHD flow. Appl. Math. Comput., 153: 645-649.
24. Ashraf, M., M.A. Kamal and K.S. Syed, 2009. Numerical study of asymmetric laminar flow of micropolar fluids in a porous channel. Computers and Fluids, 38: 1895-1902.
25. Ashraf, M., M.A. Kamal and K.S. Syed, 2009. Numerical simulation of a micropolar fluid between a porous disk and a non-porous disk. Appl. Math. Modell., 33: 1933-1943.
26. Ashraf, M., M.A. Kamal and K.S. Syed 2009. Numerical investigations of asymmetric flow of a micropolar fluid between two porous disks. Acta Mechanica Sinica, 25: 787-794.

27. Gerald, C.F., 1974. Applied Numerical Analysis, Addison Wesley Publishing Company, Reading Massachusetts.
28. Milne, W.E., 1953. Numerical Solutions of Different equations, John Willy and Sons, Inc. New York.
29. Hildebrand, F.B., 1978. Introduction to Numerical Analysis, Tata Mc Graw Hill Publishing Company Ltd.
30. Syed, K.S., G.E. Tupholme and A.S. Wood, 1997. Iterative solution of fluid flow in finned tubes. In C. Taylor & J.T. Cross (Editors), Proceeding of the 10th International Conference on Numerical Methods in Laminar and Turbulent Flow, pp: 429-440, Pineridge Press, Swansea, UK, pp: 21-25.
31. Deuflhaard, P., 1983. Order and step size control in extrapolation methods. Numerische Mathematik, 41: 399-422.
32. Lok, Y.Y., N. Amin and I. Pop, 2006. Non-orthogonal stagnation point flow towards a stretching sheet, Int. J. Nonlinear Mech., 41: 622-627.